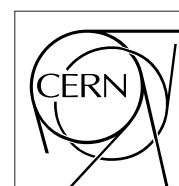**The Compact Muon Solenoid Experiment**

CMS Note

Mailing address: CMS CERN, CH-1211 GENEVA 23, Switzerland

January 18, 1999

CMS Forward-Backward MSGC milestone

O. Bouhali, J. Stefanescu, F. Udo, W. Van Doninck , L. Van Lancker, C. Vander Velde, P. Vanlaer, V. Zhukov,
K. Bernier, W. Beaumont, T. Beckers, J. De Troy, C. Van Dyck, I. Boulogne -
IIHE ULB/VUB Brussels, UCL Louvain-la-Neuve, UIA Antwerp, UMH Mons
M. Bozzo - CERN,
V. Chorowicz, D. Contardo, R. Haroutunian, L. Mirabito, G. Smadja, S. Tissot - IPN Lyon,
F. Drouhin, B. Schwaller, Y. Benhammou, F. Jeanneau, J.-C. Fontaine - UHA Mulhouse,
P.G. Verdini - INFN Pisa,
S. Barthe, A.M. Bergdolt, J.M. Brom, J. Coffin, J. Croix, H. Eberlé, W. Geist, U. Goerlach, J.M. Helleboid,
M. Hoffer, C. Hoffmann, D. Huss, P. Juillot, M.R. Kapp, M. Krauth, A. Lounis, C. Maazouzi, I. Ripp,
C. Racca, M.H. Sigward, J.P. Schunck, G. Schuster, T. Todorov, R. Wortmann, A. Zghiche -
IReS Strasbourg,
S. Bachmann, F. Beißel, C. Camps, V. Commichau, G. Flügge, K. Gundlfinger, K. Hangarter, R. Ischebeck,
J. Kremp, K. Lübelsmeyer, D. Macke, A. Nowack, D. Pandoulas, M. Petertill, O. Pooth, P. Schmitz, R. Schulte,
A. Schultz von Dratzig, R. Siedling, H. Szczesny, M. Tonutti, B. Wittmer -
RWTH Aachen I & III,
M. Ackermann, S. Atz, P. Blüm, S. Junghans, K. Kärcher, D. Knoblauch, M. Kräber, R. Metri, Th. Müller,
D. Neuberger, A. Pallares, E. Ruoff, A. Sauer, H.J. Simonis, W.H. Thümmel, S. Weseler - IEKP Universität
Karlsruhe,
V. Aulchenko, B. Baiboussinov, A. Bondar, V. Nagaslaev, L. Shekhtman, A. Tatarinov, V. Titov -
Budker Institute for Nuclear Physics, Novosibirsk.

Abstract

The CMS MF1 milestone was set in order to evaluate system aspects of the CMS forward-backward MSGC tracker, to check the design and feasibility of mass production and to set up assembly and test procedures. We describe the construction and the experience gained with the operation of a system of 38 MSGC detectors assembled in six multi-substrate detector modules corresponding to the geometry of the forward-backward MSGC tracker in CMS. These modules were equipped with MSGCs mounted side by side, forming a continuous detector surface of about 0.2 m^2. Different designs were tried for these modules. The problems encountered are presented with the proposed solutions. Operation conditions for the 38 MSGCs are reported from an exposure to a muon beam at the CERN SPS. Gain uniformity along the wedge-shaped strip pattern and across the detector modules are shown together with the detection efficiency, the spatial resolution, alignment and edge studies.

1 Introduction

The outermost part of the CMS tracker will be equipped with MSGCs. In the forward-backward region they are arranged on disks perpendicular to the beam pipe. Eleven such disks are foreseen on either side of the MSGC barrel, covering the radial region from 700 mm to 1160 mm and extending in z from $\pm$ 1215 mm to $\pm$ 2760 mm. On these disks the MSGC counters are arranged in four rings made of modules containing several MSGC counters put side by side in a common gas volume. A full description of the CMS forward-backward MSGC tracker can be found in reference [1].

The main design criteria are a full radial coverage of the entire forward-backward area for each disk, minimization of dead space between the detector modules, rigidity of the disk assembly consistent with material budget constraints, and access for services. To fulfill these criteria, two different approaches have been investigated: the so-called "open" and "closed" designs. They are briefly described in section 3 after a description of the individual counters in section 2

The aim of the forward-backward MSGC milestone was to learn how to build such detector modules, keeping in mind the future mass production and to compare the various designs. The most important problems and difficulties encountered in the construction and in the operation of the modules are described in section 4. Another aspect of the test was to learn how to run all these modules together and study the uniformity of the response. For that purpose the six detector modules were operated at the CERN SPS in the X5 muon beam. The experimental set-up is described in section 5 and the data analysis procedure in section 6. The results are presented in section 7 before drawing the conclusions.

2 Description of the MSGC counters

2.1 Substrates

As it is convenient for pattern recognition, the anode and cathode strips point towards the beam pipe in single sided counters. A trapezoidal shaped electrode geometry is chosen. The anode width is kept constant. In order to keep a constant gain over the full length of the substrate, both the anode-cathode gap and the cathode width vary with the radial position on the detector module, following an homothetic rule proposed by NIKHEF [2]:

$$G = P/8 + 20\mu\mathrm{m},\tag{1}$$

where G represents the anode-cathode gap and P the anode pitch.

For the present beam test two wedge-shaped masks have been designed, at IReS Strasbourg and at BINP Novosibirsk, corresponding to the outermost and innermost rings respectively. Their characteristics can be found in table 1. As an example, the mask layout for the outer ring is shown in Fig. 1.

	outer ring	inner ring
number of anodes	512	512
anode pitch	250 to 212 μm	200 to 185 μm
anode width	10 μm	7 μm
cathode width	139 to 110 μm	100 to 90 μm
cathodes grouped by	16	16
anode cathode distance	51 to 46 μm	47 to 44 μm
central anode length	170 mm	40 mm
total length	186 mm	52 mm
large base width	128 mm	102 mm

Table 1: Characteristics of the masks for the MF1 milestone

The final substrate material for the forward-backward MSGCs is forseen to be DESAG 263 glass, 300 μm thick, coated with a layer of semiconductive glass. The strip material will be gold deposited on a titanium adhesion layer. Such substrates meet the specifications defined for the CMS "performance prototype" [1].

For the present milestone, aiming only to test the system aspects, cheaper substrates than the final ones were used.
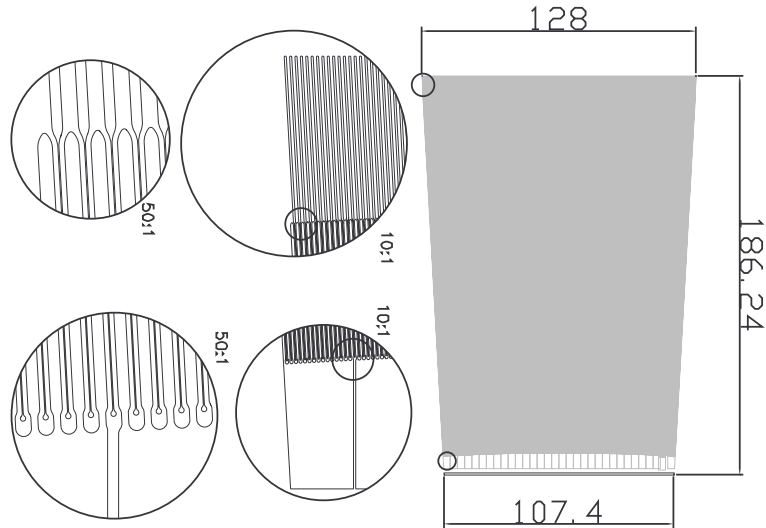
Figure 1: Dimensions in millimetre of an MSGC substrate and detailed view of the artwork at the edges of the active area.

Either aluminium or gold strips were printed on bare DESAG 263 glass by various manufacturers: SRON [3], VOSTOK [4], OPTIMASK [5], IMT [6] as shown in the first column of table 2.

company	strip material	errors on mask	yield	number of substrates	number of anodes	broken anodes	shorts
IMT	0.5 μm Au	0	84%	25	12800	30 (0.2%)	5 (0.04%)
OPTIMASK	0.8 μm Al on 0.15 μm NiCr	0	68%	32	16348	430 (2.6%)	3 (0.02%)
SRON	0.8 μm Al on 0.2 μm Cr	13 br. 3 sh.	80%	13	6656	169+20 (2.8%)	3-5 per subst.
VOSTOK	0.5 μm Au	0	80%	10	5120	250 (4.9%)	10 (0.2%)

Table 2: Statistics on the quality of MSGC substrates provided by the various plants for this test.

2.2 Drift planes

For one detector module of the outer ring (see section 3.3), the drift plane was made of a 3 mm thick honeycomb structure made of NOMEX (ARAMIDE) skins and 0.8 mm glass fibers, coated with 1.2 μm of copper and 1.2 μm of nickel. For the four other outer ring modules, it consists of 300 μm thick DESAG 263 glass, coated with a 5 nm chromium layer. Chromium was chosen for its good adhesion to glass. The layer was made so thin to obtain transparent drift cathodes to allow an optical alignment of the counters in the case of the "open" design.

It appeared that the latter type of drift planes prevents stable operation at more than 2.7 kV on the drift electrode, instead of 3.7 kV for the former type, even in the low intensity X5 beam. This is due to the high resistance offered by the thin layer of chromium, leading to charge accumulation, discharging suddenly. This behaviour is observed for both types of module designs, "open" and "closed". Although full efficiency can be obtained at 2.7 kV, as will be shown later, this lower voltage was considered as a drawback as it implies higher cathode strip voltages. Since the milestone test described in this note, new drift planes coated with 20 μm of gold have been produced and tested successfully in the X5 beam test, in June 1998, in an "open" detector module. These new drift planes hold 3.8 kV without any problem.

For the inner ring module, the drift plane was also made on 300 μm thick DESAG 263 glass but coated with a 50 nm nickel layer providing a low enough resistivity, $\sim 1\Omega$ across the plate. However the metal layer had sharp edges preventing to reach the required drift voltage.

2.3   Electrical connections

The electrical connections are made by means of two ceramic hybrids situated on each side of the strips and a service board module.

On the hybrid at the large side of the trapezoidal counters the readout chips were mounted and connected to the anodes. As the final chip foreseen for the readout of MSGCs in CMS is not yet available, the counters were equipped with four PreMux128 chips [7] per substrate. These chips hold 128 preamplifiers and shapers with 45 ns shaping time combined with a 1 MHz multiplexer. The readout hybrid had to be specially designed for the MF1 milestone and completed by a service board. The design was made at BINP Novosibirsk, the production of the PreMux128 hybrids was carried out at CERN and the service boards were produced at IEKP Karlsruhe.

The hybrid at the short side of the counters brings the high voltages to the drift plane ($\sim$-3 kV) and to the cathode strips ($\sim$-530V), by groups of sixteen. This hybrid holds protective resistors (4.7 MΩ) for the cathode groups, an high voltage filter with 4.7 MΩ resistor and decoupling capacitors (1000 pF, -2 kV). These hybrids have been designed and realized at IReS Strasbourg. Some counters had fuse resistors integrated in the bonding pads of the pitch adaptors at the input of the PreMux128 chips. These were ment to allow remote disconnection of anode strips developing a short during operation, by applying a positive voltage through a high voltage diode bypassing the cathode group protection resistor. The fuses have a resistor of $\sim$400 Ω and constitute an additional impedance at the input of the PreMux128. More details on the electronics of the present milestone can be found in reference [8].

3   The detector modules

Several trapezoidal MSGC counters are placed side by side in a common gas volume to form a detector module. In two setups, it was shown that it is possible to operate safely, counters with their neighbouring anodes as close as 400 μm and that no loss of efficiency is observed for minimum ionizing particles traversing the region between the two counters [9, 10]. Placing detector modules containing several adjacent counters in rings, should produce dead space in ϕ only between modules, not between the counters inside a module, with a minimum material budget.

Different designs have been investigated for these detector modules and six of them were built by different institutes: Aachen, Belgium, Karlsruhe, Lyon, Novosibirsk and Strasbourg. Four modules (O1 to O4) have been built following the so-called "open" design (see section 3.1), one module (C1) follows the "closed" design (see section 3.2) and the sixth module (C2) is a variant of the "closed" design (see section 3.3). All modules have outer ring substrates except module O4, having inner ring substrates.

3.1   The open design

A full description of the "open" design can be found in [11]. Its main characteristic is to build and test complete MSGC counters including their electronics before mounting and aligning them inside a module. During the entire assembly and test procedure of the individual counter, all parts remain accessible for intervention and even replacement. For the present milestone, eight counters were enclosed in each "open" module, except for O4 containing only two counters.

3.1.1   The gas box

The gas box bottom plate consists of an aluminium carbon fiber honeycomb composite, while the curved edges are made of aluminum tubes with a rectangular section of 3×10 mm^2 and a wall thickness of 200 μm. These are used as integrated gas distribution manifolds, the gas mixture being delivered via laser-drilled holes facing every MSGC inside the box. The radial edges are made of PEEK profiles. The gas box is finally sealed by an aluminized kapton foil glued on top of the frame (see fig. 2).

3.1.2   The individual MSGC counter

Each counter is made of one substrate, one drift cathode, one front-end electronic hybrid and one high voltage hybrid (see fig. 3). They are mounted stress-free inside the box with three excentrics. They are visually aligned through the transparent drift plane, by means of fiducial marks on the central cathode. The front end chips rest in thermal contact with a water cooling circuit, made of a thin wall aluminium tube, identical to the ones used for the gas manifolds, glued on the gas box honeycomb plate.
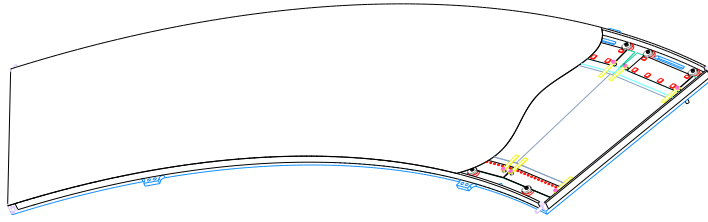
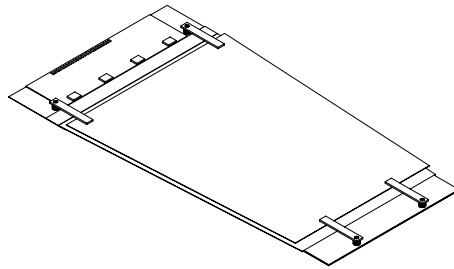Figure 2: An "open" design detector module.

Figure 3: An MSGC counter of an "open" design module.

3.2 The closed design

As this design was finally choosen by the CMS management in December 1997, it is described in detail in the tracker Technical Design Report [1]. In this approach, four substrates are glued to a stiff frame. The detector module is closed before the front end electronic hybrid is connected to the substrates. Thus the exposure time of the substrates is minimized.

A detector module consists of three frames supporting the substrates, the drift cathodes and the electronic hybrids (see fig. 4). For the present test, the frames were machined out of full material; for the bottom and top frame, Stesalit was used, while the middle frame was made of PEEK, avoiding splinters from the Sresalit on the substrates.
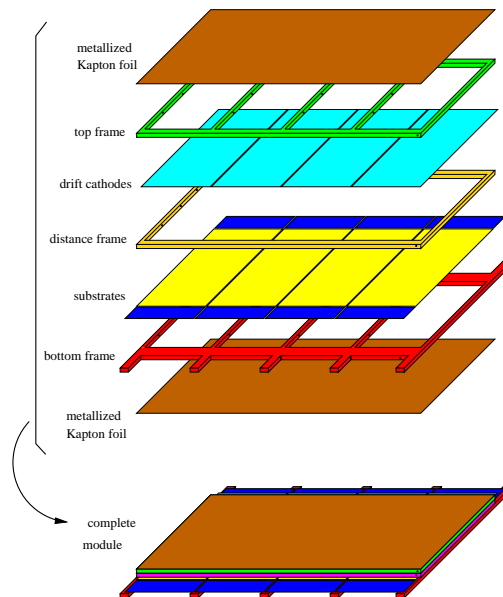

Figure 4: The various elements building up a "closed" design module.

The substrates are glued to the 2.5 mm thick bottom frame after relative alignment. The alignment procedure is described in detail in reference [1]. Stiffening bars inside the frame are foreseen to avoid deformation of the sub-

5

strates through sagging. Holes in these bars allow the counting gas to pass through. The distance frame, without any internal bars, separates the substrates and the drift cathodes. With a 3 mm height it defines the sensitive detection volume. It is glued onto the bonding pads of the substrates, which are bonded to the readout and high voltage hybrids outside the gas volume. The cooling of the readout electronics was not implemented on this milestone prototype. The top frame supports the drift cathodes. The entire module is closed by a Kapton foil that is coated with copper on the outside. A cross section of a module is shown in figure 5. For the present milestone, the C1 module
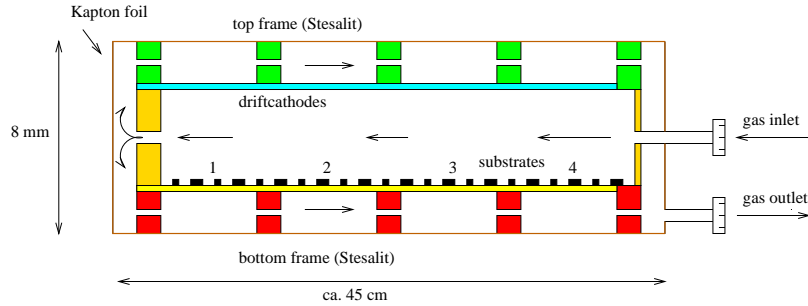

Figure 5: Cross section of a "closed" design module.

is made of two such modules mounted side by side on the same aluminium plate support, leading to eight substrates in total for C1 also.

3.3 A variant of the closed design

Another design, similar to the "closed" design described above, is illustrated in Fig. 6. Here the gas volume is closed by the drift plane itself. Therefore it consists of a 3 mm thick metallized carbon fiber honeycomb structure. An attractive feature of this design is the large radiation length of carbon fiber composites, as compared to glass used for the other drift planes. Details on the particular design can be found in reference [12]. Module C2 has only one module with four substrates.
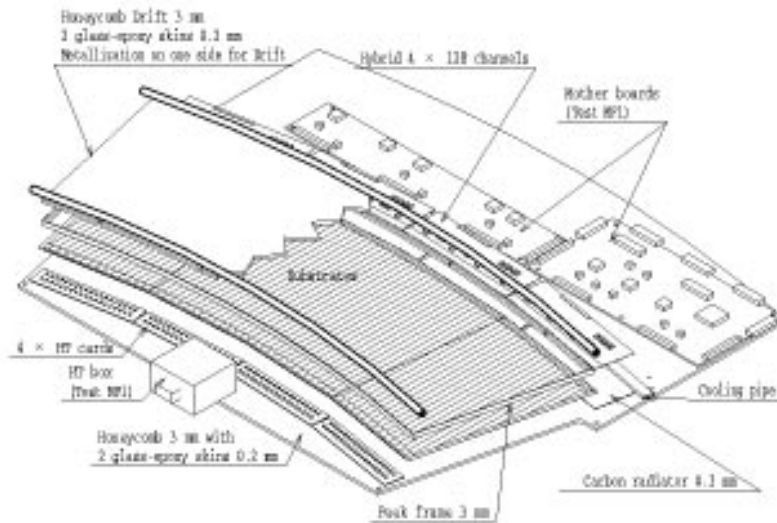

Figure 6: Scheme of the module following a variant of the "closed" design.

4   Outcome of the construction and operation of the modules

Prior to assembly into the detector modules, the MSGC substrates were optically inspected to record interrupted or shorted anode strips. Electrical tests using probe stations were also used in some cases. The results of this inspection can be found in table 2 showing the numbers of defective strips on the substrates produced by the different plants, together with the total numbers of substrates and anodes produced. In the case of SRON, most defects are due to errors already existing on the mask provided by OPTIMASK, which brings the quality of their production almost to the very good level of IMT. The two other plants, less experienced, still need to improve their yield.

For the "open" design, where the substrates are connected to the readout electronics before module assembly, a high voltage test was performed in a nitrogen atmosphere. Every MSGC counter was brought to 80% of the operation voltages before installation into the common gas box. For the "closed" design the connection to the readout electronics was only executed after module assembly. Anodes leading to problems in the subsequent high voltage test were disconnected by removing the corresponding bonding wire.

Some detector modules had diodes bypassing the 4.7 MΩ protection resistor at the input of the groups of 16 cathode strips. These diodes were supposed to conduct only a positive bias voltage applied to blow the resistor fuse through the short, for the counters equipped with fuses. Also some counters of the "open" design modules had these diodes mounted, even if they had no fuses. Erroneous reverse mounting of these diodes prevented to test properly the fuse system and made these "open" design detector modules more vulnerable since the protection resistors to the cathode groups were bypassed in normal operation conditions. This situation prevents us to draw conclusions on the robustness of the strips and preamplifiers during this beam test.

During the initial testing of one of the open design module (O1), a flush rate of five times the nominal one was used. When starting up the cooling circuit this led to DME condensation due to the combined effect of the cooling and the excessive flush rate in this high impedance gas distribution. As the voltages were on during that cooling test, the shorts produced by the small DME droplets in conjunction with the reversly mounted diodes bypassing the protection resistors, simultaneously damaged about 20% of anode strips, distributed everywhere in this detector module. For this reason the next "open" modules were built with larger holes for the gas inlet.

During the mounting procedure of the first 4-fold "closed" design C1 half module, severe problems were encountered while aligning the three different frames one over the other, leading to a misaligned module with gas leak problems. In a gas leak search operation, water entered the module and caused areas with shorts leading to about 30% of broken strips. After these experiences the mounting procedure was improved and the second C1 half module was built with only a few damaged strips .

For module O3, the recommended cleaning procedure of the substrates was not followed. Residuals from the production procedure resulted in high currents driven by these substrates, leading to significant voltage drops and poor performances of the O3 counters. Proper cleaning of one of the O3 counter after the beam test brought it to performances comparable to these of the good counters.

More details concerning the module assembly and tests performed during the construction can be found in reference [8], both for the "open" and "closed" design.

5   Experimental set-up

The six MSGC detector modules were tested in a tertiary 100 GeV/c muon beam, obtained from the primary SPS proton beam at the CERN X5 beam facility [13]. Beam particles were selected by means of a scintillator trigger and their trajectory reconstructed in two orthogonal directions (X and Y) thanks to a silicon microstrip telescope. Figure 7 shows the experimental set-up consisting of two mechanically independent benches, one carrying the six MSGC detector modules and one carrying the telescope, the trigger scintillators and other silicon detectors under test for the CMS tracker (not used in this note and shown in white on figure 7). The reference frame used in this paper is also shown on figure 7, with the Z axis along the beam direction, the X axis vertical and the Y axis horizontal; the various detector planes are, in first approximation, parallel to the XY plane.

The trigger is performed by a coincidence of two out of three scintillators. The first one is always a 12×12 cm^2 scintillator and the second one is either a 6×6 cm^2 or a 2×2 cm^2 scintillator.
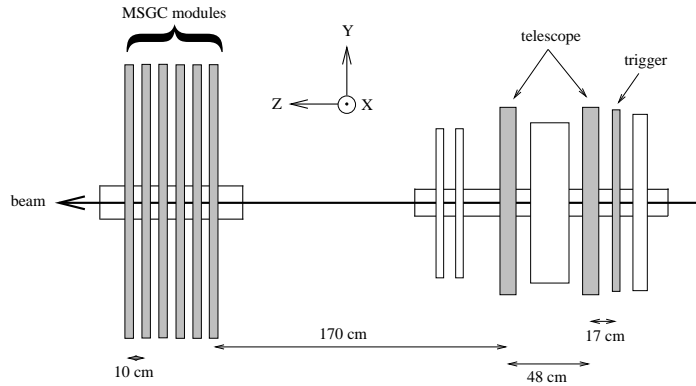
Figure 7: Top view of the experimental set-up with the definition of the reference frame. The boxes left in white are other silicon detectors under test for the CMS tracker, not used in this note.

5.1 MSGC detector modules layout

A special support structure has been designed and built at IReS Strasbourg to hold the six forward MSGC detector modules, as shown in figure 8. Each MSGC module is individually mounted on a 6 mm thick aluminium plate
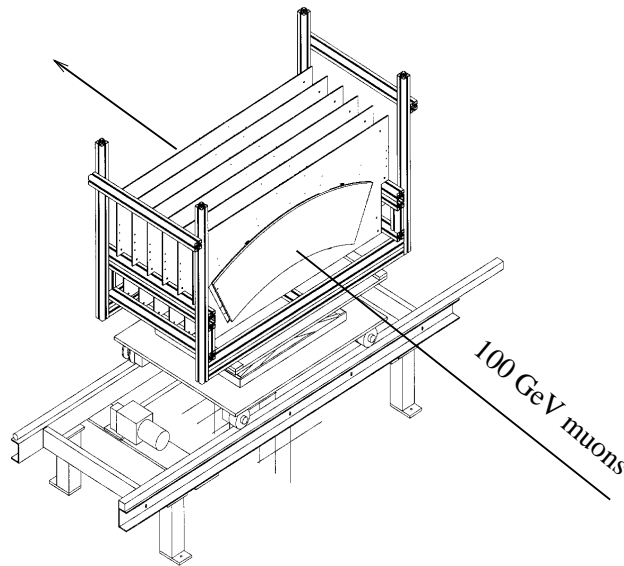

Figure 8: Perspective view of the bench with the six MSGC detector modules.

supporting also the gas and cooling connectors, the high voltage lines and the electronics service boards. The aluminium bare plate had a hole of the size and shape of the detector module milled in it behind each module, to limit multiple scattering. As can be observed on figure 8, the modules are mounted in such a way that the counters have their strips roughly parallel to the X axis and perpendicular to the Y axis. In fact, due to the trapezoidal shape of the MSGC counters, this is only true for one strip in each module, somewhere in its middle.

The whole platform is mounted on a movable support enabling translations of the six modules together, in X and Y directions. The steps are 1 mm by one turn of a screw for X and 1.5 mm by one turn in Y. The precision or control of these motions are rather poor. The maximum excursion allows to scan a whole MSGC module, with a total possible translation of 32 cm in X and 110 cm in Y.

8

A photograph of the MSGC bench during the beam test is shown on Fig. 9.

The six modules were flushed in parallel with a gas mixture of Ne/DME-30/70% delivered by a single gas rack. Although the water cooling pipes were mounted in some of the modules, they were not used during the beam test. For the present milestone, the high voltage for the cathode strips were connected separately to each individual MSGC counter. For the drift high voltage of the "open" design modules, there were three lines per module, one line for each of the two edge counters and the third line for the rest of the counters. In the case of the 4-fold "closed" design half modules there is one drift voltage line per 4-fold module.
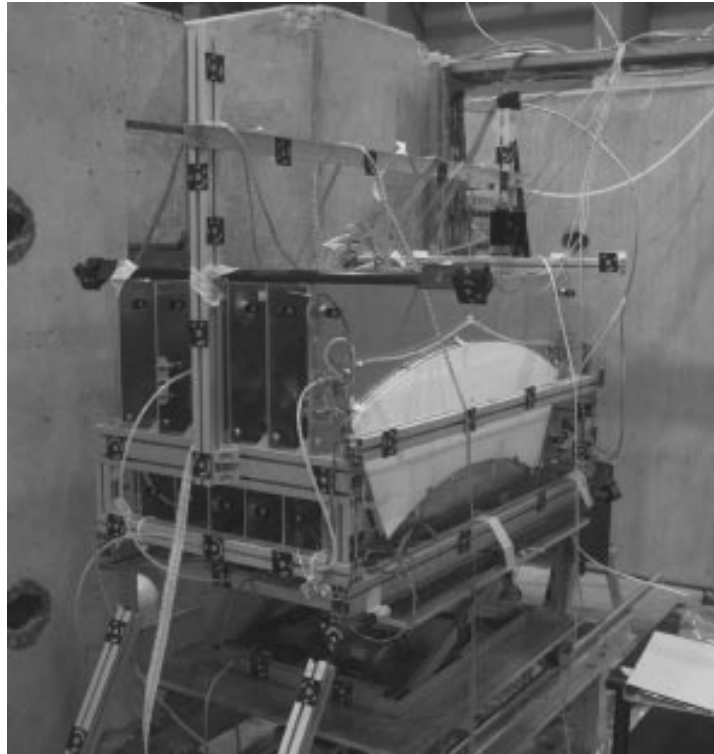

Figure 9: Photograph of the bench with the six MSGC detector modules.

5.2   Telescope layout

A silicon microstrip telescope, built in Bari [14], was used to reconstruct in space the trajectory of triggered beam particles. It consists of four double sided silicon microstrip detectors with $50 \, \mu$m readout pitch, gathered in two arms of two detectors. These detectors are $300 \, \mu$m thick each, with 384 readout strips on each side, crossed at $90°$. The readout is done using VIKING multiplexer chips [15]. On the p side, measuring the Y coordinate, an intermediate p^+ strip is implanted between two readout strips, in order to improve the linearity of the charge collection whereas on the n side, measuring the X coordinate, a p-stop strip is inserted in between two readout strips, to avoid charge spread. As a result of this asymmetry between the p and n sides, the spatial resolution on the Y coordinate is expected to be better than this of the X coordinate.

Unfortunately, as during the present tests the silicon telescope and the MSGC modules were on different benches, they underwent uncorrelated vibrations, especially during working hours. The situation is very unfavourable to an alignment of the two systems. This situation is made still worse by the geometry of the set-up (see fig. 7), with a small distance between the two telescope arms and a large distance between the telescope and the MSGC detector modules.

5.3   Data acquisition

The data acquisition was performed by a distributed system implemented by GRPHE Mulhouse. It is an updated version of the system described in [16]. For the sake of performance and modularity the system's hardware is di-

vided into a front-end and an event builder part. The front-end part itself is segmented into three VME crates which communicate with the event builder via a daisy chained fast data link.

During beam spills, the multiplexed analog output of the detector front-end electronics is digitized, demultiplexed and stored by means of several VME FADC modules which reside in the front-end crates. The readout cycle is controlled by one VME sequencer module per crate which provides the timing signals for the front-end electronics and the FADCs. A detailed description of these two modules can be found in [17]. For the triggering of the whole system, custom designed modules are used [18]. All front-end crates are equipped with a real time processor running OS9 which starts the readout cycles, collects the data from the FADC modules and rearranges it for transmission to the event builder.

The event builder tasks are distributed over two different processors residing in the same VME crate. A real time processor running LynxOS synchronizes the acquisition in the different front-end crates, creates ZEBRA format data banks [19] and transfers them to a dual port memory. From there a Themis SPARC processor writes them to disc and sends them asynchronously via ethernet to the CERN Central Data Recording. During the beam test, an acquisition performance of 75 events per spill was achieved (a spill delivers approximately 15,000 muons in 2.5s). To reach that rate, due to the large number of silicon detectors also under test, only the two MSGC counters in each module that were in the beam, were read out. However, a few runs were successfully taken reading out the 38 MSGC counters together.

An online monitor task running on a Unix workstation collects portions of the data from the event builder RTPC (Real Time Processor Card) via a dedicated interface. This data is visualized using PAW. The monitoring program was written by IPN Lyon.

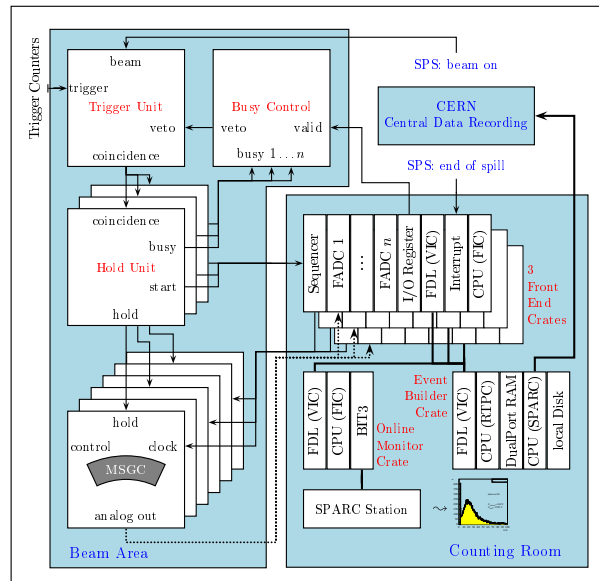Figure 10 shows a schematic diagram of the whole DAQ system.

Figure 10: Schematic diagram of the distributed DAQ system

A Slow Control Module [20] in a separate VME crate communicates with the MSGC front-end electronics via a serial bus. This allows the monitoring of PreMux128 supply voltages and temperatures as well as the control of PreMux128 output signal offsets.

6   Data analysis procedure

6.1   MSGC data analysis

In addition to the charge possibly deposited by an ionizing particle, the raw values given by the ADC channels contain contributions from the channel pedestal and from a common mode fluctuation, different for each event. The raw data ADC count for the ith strip in the kth event can be written as:

$$ADC_i^k = S_i^k + P_i + C_i^k$$

where S_i^k is a possible signal due to an incident particle on strip i in event k, P_i is the pedestal of the ith ADC channel and C_i^k is a common mode shift of a group of channels including channel i, for the kth event.

The retrieval of the particle related signal from raw data requires a subtraction of the pedestals and a correction for the common mode shifts. The pedestals were computed for each ADC channel as the average charge value for the 500 first events of the run. An iterative procedure was used in order to reject events in which the considered strip may have been hit by a particle. After correction of the raw data for the pedestals, the common mode was computed for each event, separately for groups of 128 strips physically connected to the same readout chip. It is given by the average charge value for the group of strips considered.

After these two corrections, the strip noise σ_i was estimated as the standard deviation of the distribution of the remaining signal S_i, in the absence of an incident particle. Figure 11 shows the strip noise for each channel in two typical MSGC counters of module O2. The average noise is of the order of 9 ADC counts. A few spikes corresponding to slightly noisy strips are observed together with some dips corresponding to strips damaged either during the construction of the modules or during operation (see paragraph 4). Dead and noisy channels were rejected from subsequent analysis. The channels were identified as dead if their noise is less than half the average noise, as noisy if it is more than five times the average noise.
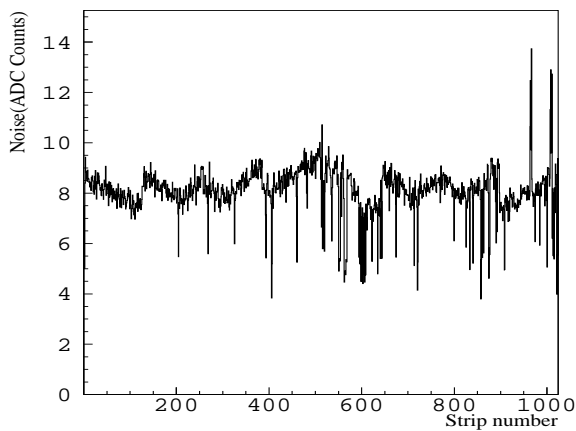

Figure 11: Strip noise versus channel number for two typical MSGC counters.
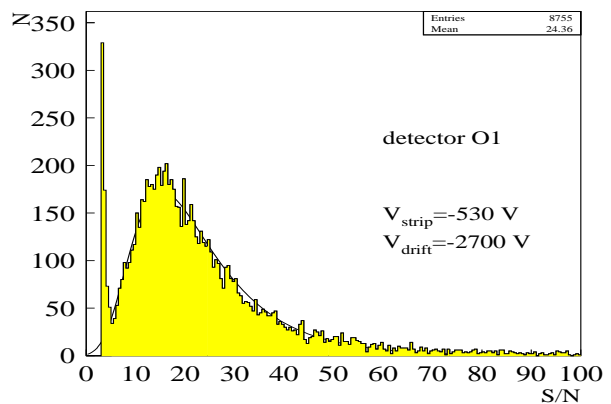
Figure 12: Typical signal over noise distribution for an MSGC counter.

To find impact points of ionizing particles with the MSGC counters, clusters of strips with a signal were formed. A strip is considered to have a signal if $S_i/\sigma_i > 3$. Adjacent strips satisfying this criterion were added together till no more adjacent strips above threshold were found. To allow for dead strips, one strip below threshold was accepted within a cluster. The cluster charge $Q^{cluster}$ was computed as the sum of the signals of the strips accepted in the cluster. The cluster noise $\sigma^{cluster}$ was defined as:

$$\sigma^{cluster} = \sqrt{\sum_{i=1}^{N} \sigma_i^2}, \tag{2}$$

where N is the number of strips belonging to the cluster. The cluster signal to noise ratio was then defined as:

$$S/N = Q^{cluster}/\sigma^{cluster}. \tag{3}$$

Figure 12 shows a typical signal to noise distribution obtained for one of the MSGC counters operated on the efficiency plateau with a drift voltage of -2700 V and a cathode strip voltage of -530 V. One can clearly see the separation between noise and signal. In order to reject the noise clusters observed on figure 12, a cluster was eventually accepted if its signal to noise ratio exceeds 5. This distribution corresponds to an average signal over noise ratio of about 24, after the cut rejecting noise clusters. It should be pointed out that the definition of the signal over noise ratio adopted in this note is not the one usually used by the CMS MSGC community. In the latter case only the noise of a single strip is taken into account. As a result, before comparing it with our estimation, it should be divided by the square root of the average number of strips per cluster. The average cluster size was typically 2.3 strips for the present milestone (see section 7.7).

11

A coordinate of the incident particle impact point can be given, in strip number, by the charge centre of gravity method:

$$n_{strip} = \frac{\sum_{i=1}^{N} n_i S_i}{\sum_{i=1}^{N} S_i}, \tag{4}$$

where n_i is the order number of the ith strip in the cluster.

Due to the trapezoidal shape of the counters leading to varying anode pitches, knowledge of the coordinate along the strips is needed to transform n_{strip} into a spatial coordinate. For this purpose use will be made of the information provided by the silicon telescope as there are no MSGC stereo strips in the present prototypes.

6.2 Telescope data analysis

As pointed out in the preceding paragraph, the silicon telescope information is needed to calculate a spatial coordinate for the impact points measured by the MSGC counters.

Pedestal and common mode corrections together with cluster finding are performed in a way similar to the one used for MSGCs. However no strip with a signal below the strip threshold is accepted within a cluster and the cluster signal to noise ratio must exceed 15. In order to avoid ambiguities, events with more than one cluster in a telescope plane were rejected.

Before reconstructing the trajectory of beam particles, the telescope planes needed to be aligned. The first double sided silicon detector encountered by the beam (right side of fig. 7) was assumed to have its p and n side strips perfectly aligned respectively with the X and Y axes of the reference frame. For the three other detectors, the p and n side strips measure local y and x coordinates. To go from these local xy frames to the XY frame, a translation along the X and Y axes may be needed as well as a rotation around the Z axis. Shifts of the Z coordinates given by the geometer are also investigated. The estimation of these parameters for the changes of reference frames are done using an iterative procedure.

In a first step, no rotation and no Z shifts are assumed. Initial values for the translations in X and Y are obtained for detectors 2, 3 and 4 by requiring that the average value of the X and Y coordinates of beam particles impact points in these detectors, equal those of detector 1.

These initial parameter values are used to correct the x and y coordinates measured by each detector to give X and Y coordinates. For each event a χ^2 fit to a straight line is performed in order to estimate the slope and intercept of each track in the two XZ and YZ projections.

These track parameters are then assumed to perform a single χ^2 fit for all events together in order to give a better estimation of the parameters determining the changes of reference frames. The estimations are further improved by going back to the track parameters estimation.

The distributions of the residuals obtained for the corrected X and Y coordinates, T_i^x and T_i^y ($i = 1, 4$), at the end of this iterative procedure, are shown in figure 13. The standard deviation of these distributions are of the order of 5 μm for the Y coordinate and 10 μm for the X coordinate that is less precise, as expected (see paragraph 5.2). Assuming the same spatial resolution for the four planes providing a given coordinate, these residuals correspond to resolutions of 3.5 μm and 7 μm respectively.

7 Results

7.1 Trigger timing adjustment

Before accumulating data, it was necessary to adjust the timing of the trigger signal that controls the MSGC front-end electronics and the sampling of the FADCs. For this purpose a delay box was introduced in the trigger line. Figure 14 shows the variation of the average cluster charge with the delay introduced, for two MSGC detector modules, O1 and C1. It can be observed that in both cases, the optimal delay is of the order of 20 ns. This value was used for the rest of the data taking.

7.2 Beam profiles

Figure 15 shows the beam profile observed by the two times four MSGC counters of the "closed" design module C1, for eight different positions of the module with respect to the beam. For each position, two different counters
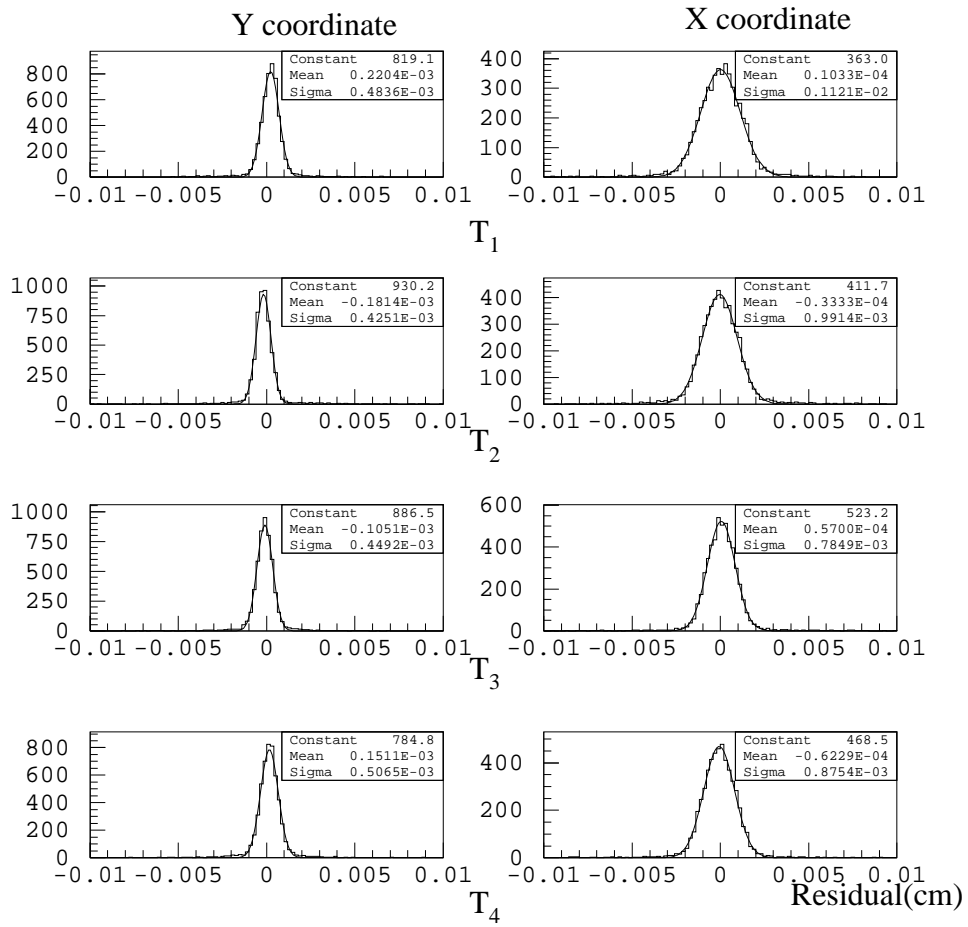
Y coordinate

X coordinate

Constant	819.1
Mean	0.2204E-03
Sigma	0.4836E-03

Constant	363.0
Mean	0.1033E-04
Sigma	0.1121E-02

T_1

Constant	930.2
Mean	-0.1814E-03
Sigma	0.4251E-03

Constant	411.7
Mean	-0.3333E-04
Sigma	0.9914E-03

T_2

Constant	886.5
Mean	-0.1051E-03
Sigma	0.4492E-03

Constant	523.2
Mean	0.5700E-04
Sigma	0.7849E-03

T_3

Constant	784.8
Mean	0.1511E-03
Sigma	0.5065E-03

Constant	468.5
Mean	-0.6229E-04
Sigma	0.8754E-03

T_4

Residual(cm)

Figure 13: Distribution of the residuals for the eight telescope planes, after alignment.

detector O1 ○
detector C1 ●
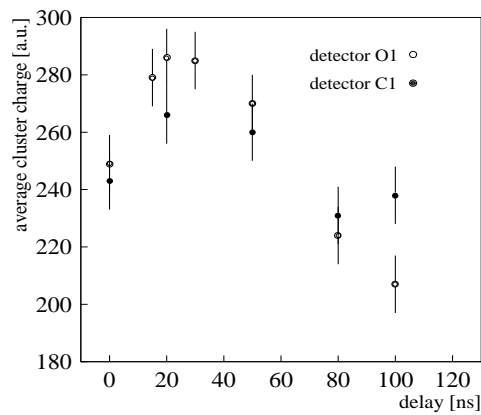
Figure 14: Average cluster charge versus trigger delay for two MSGC detector modules, O1 and C1.

13
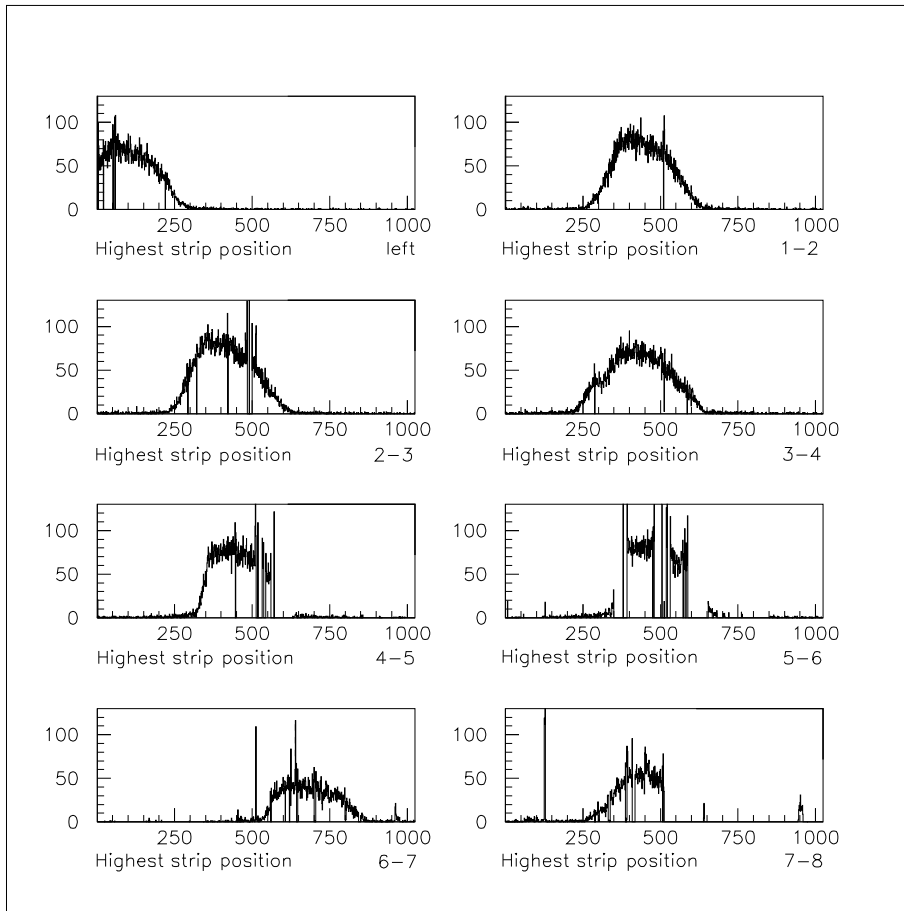
Figure 15: Distributions of the number of times that each strip has the highest charge, in two counters of the module C1. The beam scans one or two of the eight MSGC counters in C1.

are read out, those hit by the beam. The figures show for each strip of the two counters that are read out, the number of times they had the highest charge. Counters 5 to 8 show a large number of dead strips damaged during the construction (see section 4). Neighbouring strips have a higher counting rate as the ionization left by particles above a dead strip is deviated to neighbouring strips, if not dead.

7.3 Efficiency plateaus

In order to find the adequate working conditions, efficiency plateaus were measured. The particle detection efficiency of a given module is estimated taking as reference, tracks reconstructed by the eight planes of the silicon telescope. Tracks with an impact point prediction outside the MSGC sensitive area as well as those hitting a region with dead strips were rejected. A cluster reconstructed in an MSGC was accepted only if the difference, in absolute value, between the Y coordinate of the impact point with this module, calculated with the telescope information only, and the Y coordinate calculated with the n_{strip} value measured by the MSGC module, is less than a value corresponding to about 3 standard deviations of the distribution of this difference.

Before applying the above procedure it is necessary to align the MSGC detector module with respect to the telescope by requiring the distribution of that difference to have a zero mean value. This distribution is shown in figure 16 for each module, after alignment; the difference of coordinates is expressed in number of strips. The standard deviation of each distribution, expressed in μm, is displayed for each module. A slight increase from module O1 to module O4 is observed. It is due to the position of the module in the beam, module O4 having the largest distance to the silicon telescope. The distribution observed for module C1 is 20% larger, due to the fact that the beam was hitting a bad substrate (number 5), with many dead strips in this run (see fig. 15).

The diagrams in figure 17 show the detection efficiency as a function of the applied cathode strip voltage (a) and as a function of the average cluster signal to noise ratio (b), for module O1, with a drift voltage of -2500 V. A full
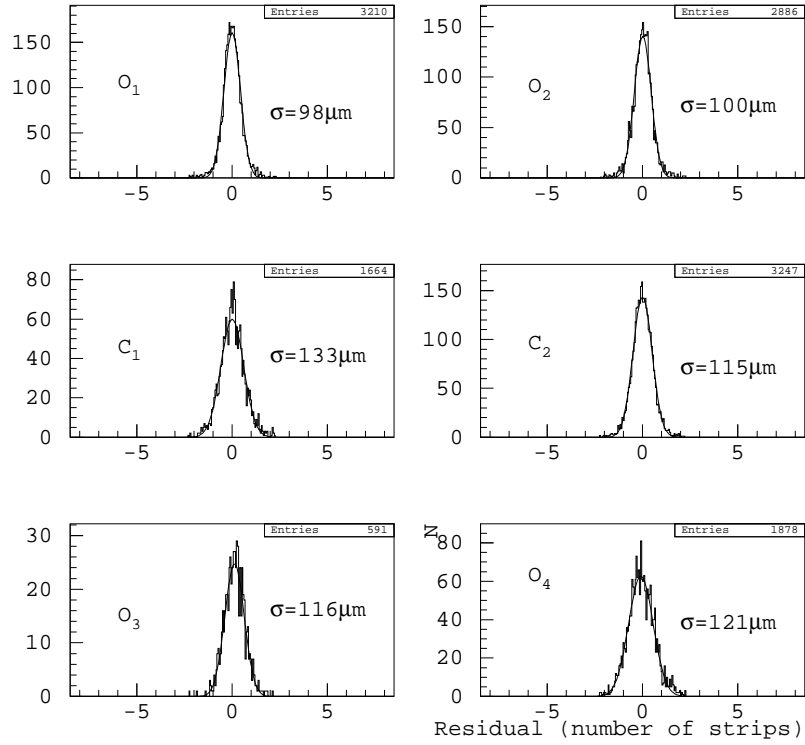
14

Figure 16: Distribution of the difference between the Y coordinate of the impact point of beam particles with the six modules, calculated with the telescope information only, and the Y coordinate calculated using the n_{strip} value measured by the MSGC module.
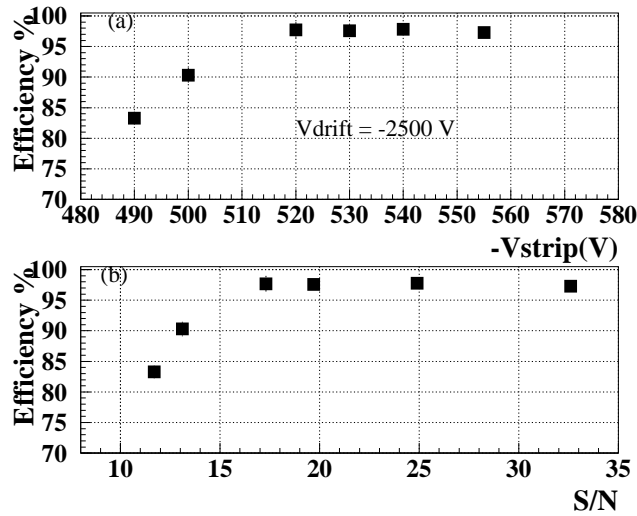

Figure 17: Detection efficiency as a function of the cathode strip voltage(a) and as a function of the cluster signal to noise ratio(b), for module O1.

15

efficiency of about 97.5% starts with a cathode strip voltage of about -520 V and an average signal to noise ratio of about 17. Similar results are obtained for other modules but the lack of statistics with the appropriate conditions to calculate the efficiency of each counter with the above procedure prevents us to show them all. To compare the uniformity of response of all counters, the signal to noise ratio, easier to calculate, will be used instead (see paragraph 7.5). Indeed, for a given gas, the efficiency plateau is expected to start at the same average S/N for all counters.

Full efficiency can be reached at a lower cathode strip voltage with a higher drift voltage. This is illustrated by figure 18 showing for module C2, the variation of the average signal to noise ratio with the drift voltage for a fixed cathode strip voltage of -530V. One point at -510V is also shown. It demonstrates that an increase of about 700 V on the drift allows to decrease the strip voltage by 20 V. This is interesting regarding possible sparks as their energy is proportional to the square of the strip voltage. A lower strip voltage thus decreases the risk of damaging the strips with sparks. Unfortunately, as explained in paragraph 2.2, only module C2 could be operated at high drift voltages in this test. However in June 1998, counters of an "open" design module could be tested in the same beam, with new
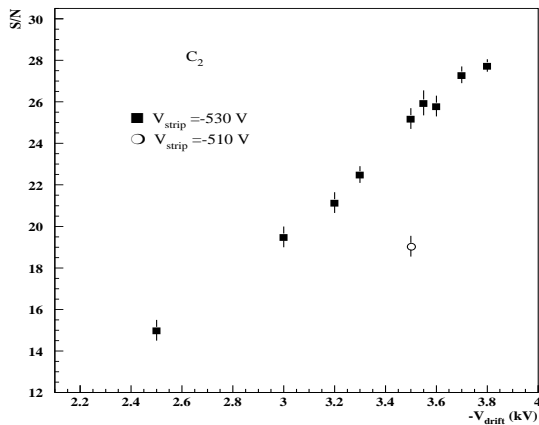

Figure 18: Average signal over noise ratio versus drift voltage for module C2 at two cathode strip voltages: -530 V and -510 V.
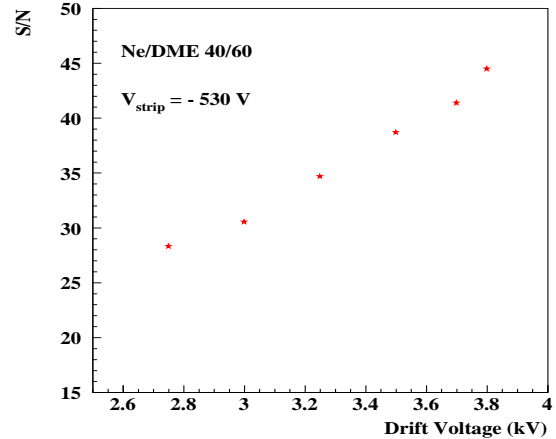
Figure 19: Average signal over noise ratio versus drift voltage for an "open" module with a new drift plane, measured during the June 1998 beam test at a cathode strip voltage of -530 V.

drift planes. Figure 19 shows the variation of the average signal over noise ratio as a function of the drift voltage for an MSGC counter of the June test. The detector was filled with a Ne/DME-40/60% gas mixture and operated at a cathode strip voltage of -530 V. A drift voltage of 3.8 kV is now also reached. It should be noted that the higher neon content in the June gas mixture is expected to lead to a higher signal to noise ratio, at the same voltages [21]. However the lower signal to noise ratio observed for C2 in figure 18 is mainly due to a higher noise (see section 7.5

7.4   Cluster characteristics

Figures 20 shows distributions of the strip multiplicity within clusters and distributions of the cluster multiplicity for one module of the outer ring(O1) and one module of the inner ring(O4). These data were taken with a drift voltage of -2700 V(-1500 V) and a strip voltage of -530 V(-510 V), for O1(O4), well on the efficiency plateau. The average cluster width is about 2.4 strips for the outer ring counter, as usual with the Ne/DME-30/70% gas mixture used here. It is significantly larger, 3.6 strips for the counter of the inner ring but one should keep in mind the smaller anode pitch for the inner ring: 190 μm in average instead of 230 μm. However translated in μm these cluster sizes amount to 680 μm for the inner ring substrates and 550 μm for the outer ring substrates, although the lower drift field in the latter case should lead to a 20% smaller transverse diffusion coefficient [21]. On average, 1.2 clusters satisfy the cluster selection criteria for each trigger, for both types of substrates. It should be noted that as only two counters per plane were read out at the same time, this corresponds to 1024 MSGC channels. This number of clusters higher than one is to be attributed mainly to true beam particles as the same cluster multiplicity distribution, taken with a random trigger, between beam spills, shows an average value of 0.05 only. Rising the thresholds does
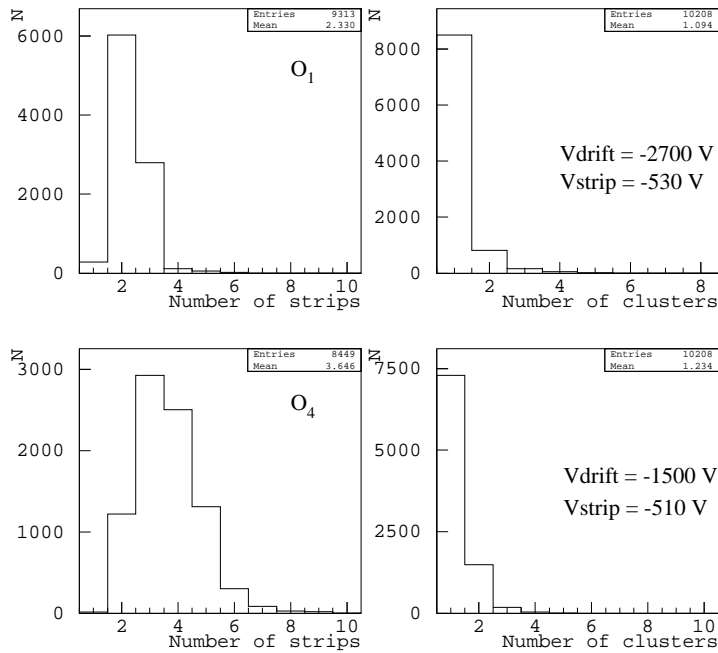
16

Figure 20: Strip multiplicity distributions within clusters (left) and cluster multiplicity distributions (right) for one outer ring counter (top) and one inner ring counter (bottom)

not decrease that number significantly but decreases the detection efficiency. It was estimated that this number of random clusters corresponds to a strip occupancy of 0.03% only.

7.5 Gain uniformity study

A careful tuning of individual high voltages for each MSGC counters, in order to reach the required gain, should be avoided in CMS. For this reason all MSGC counters were scanned with the beam in various regions of the substrates in order to check the uniformity of the response.

7.5.1 Scan along the strips

As the distance between the anodes and cathodes varies along the strips, it is important to verify that the gain does not vary too much along the strips. Figures 21 (a), (b) and (c) show the variation of the average signal to noise ratio as a function of the anode pitch, separately for the six modules.

For this scan looking at gain variations inside a given counter, it was not important to operate the different modules at the same voltages. The various operating conditions can be found on the figure. They explain most of the signal to noise variations from one module to another. However, in the case of O3, the 60% lower signal to noise ratio, is also due to the high current(a few μA) drawn by the substrates of this module, leading to a significant voltage drop in the protection resistor (see section 4). In the case of module C2, operating at a higher drift voltage than the other modules, the signal to noise ratio is still 20% lower. This is due to a bad connection to the readout electronics, leading to important common mode fluctuations and an average noise twice as large as for the other modules (see section 7.6). It should also be noted that the inner ring module O4 needs lower voltages due to the smaller anode width.

For modules shown in figures 21 (a) and (c), it is observed that the pulse height is indeed constant along the strips. The gain variations are less than 10% which is below the usual gain variation obtained from one substrate to the next for MSGCs with parallel strips. These substrates were produced by IMT, SRON and VOSTOK. On the contrary, for modules in figure 21 (b), for which the substrates were both produced by OPTIMASK, a decrease of up to 20% is observed with increasing pitch, although the larger pitches are towards the readout side (see fig. 21(b)).
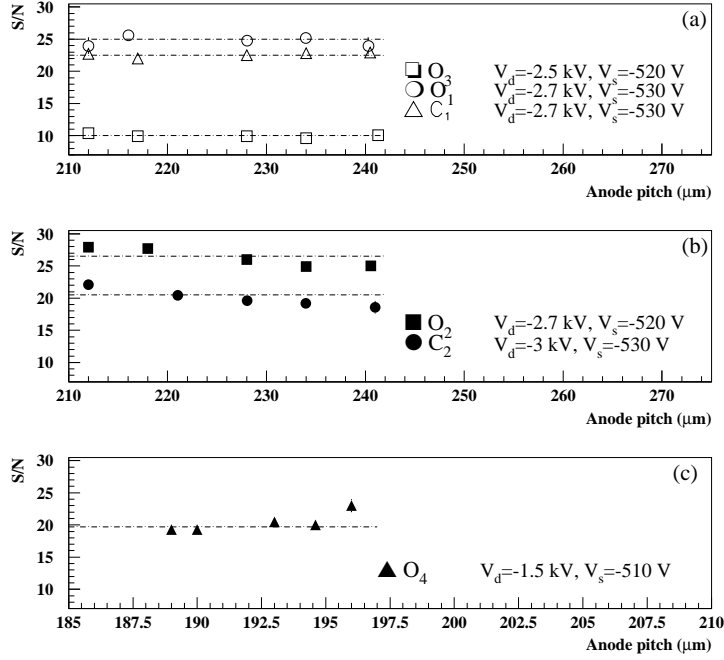
Figure 21: Average signal to noise ratio as a function of the anode pitch, for modules O3, O1 and C1(a), for modules O2 and C2(b) and for module O4(c).

7.5.2 Scan perpendicular to the strips

The uniformity of the response in a direction perpendicular to the strips was also checked. Figures 22 show the variation of the average signal to noise ratio for the eight MSGC counters of modules O1, C1 and O2, and for the four substrates of module C2. Modules O3 and O4 were not in the beam during this scan. For this scan all counters were operated at the same voltages, -530 V on the cathode strips and -2700 V on the drift plane, but module C2, operated with -3500 V on the drift plane. The different marks correspond to different positions of the beam, in each four corners of the substrates. The statistical errors on these measurements are negligible. The full lines correspond to the average value of 25 for all measurements. The dashed and dotted lines to one and two standard deviations from that mean ($\sigma = 2.8$) respectively.

For module O4, containing only one working counter, the uniformity of the signal to noise ratio has been studied as a function of the distance of the average beam impact point to the central strip of the counter (see fig. 23). The counter was operated with -510 V on the cathode strips and -1500 V on the drift plane. The gain variations observed are less than 15%.

This gain uniformity study indicates that it might be possible to operate at the same high voltages, all MSGC counters in a given module. Gain variations smaller than 25% are then expected. It should however remain possible to modify the voltages on some counters showing some defect. The relation 1, between the anode pitch and the anode-cathode gap will need to be checked and maybe adapted, depending on the substrate provider. All these results on uniformity need to be checked with coated "CMS performance" substrates and at the higher drift voltage foreseen.

7.6 Noise comparison

Figure 24 shows the variation of the average strip noise per substrate, as a function of the substrate number, for modules O1, O2, C1 and C2. As already explained, the higher noise observed for C2 is due to bad connections in the electronic service board and this reflects into the signal over noise ratio (see sections 7.3 and 7.5). The lower values observed for O2 are due to a different tuning of the FADC amplification used for that detector module. Indeed, their signal over noise ratio is the same as for O1 and C1, at the same voltages (see fig. 22).

Module O2 contains counters with and without 400 Ω resistors between the anode strips and the preamplifiers. The
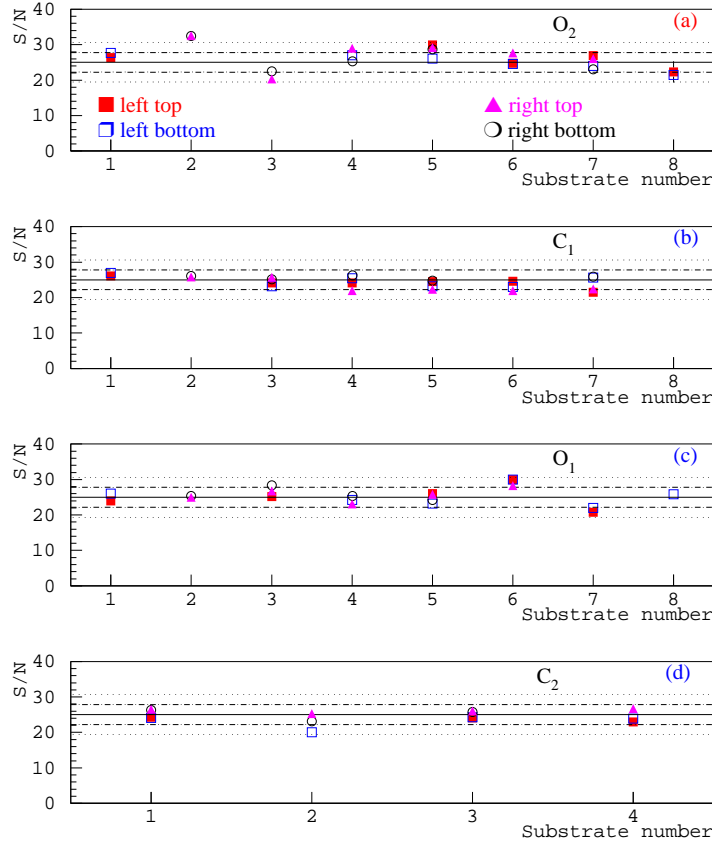
Figure 22: Variation of the average signal to noise ratio versus the counter number in module O2(a), C1(b) O1(c) and C2(c). The square(round) marks correspond to beam positions in a left(right) corner of the substrates. The open(closed) marks correspond to beam positions in a bottom(top) corner of the substrates. The full lines correspond to the average value of all measurements for the module. The dashed and dotted lines to one and two standard deviations from that mean.
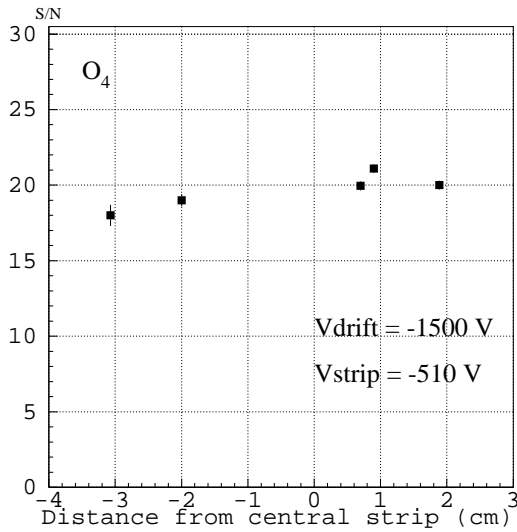

Figure 23: Variation of the average signal to noise ratio versus the distance from the average beam impact point to the central strip of the single counter in module O4.
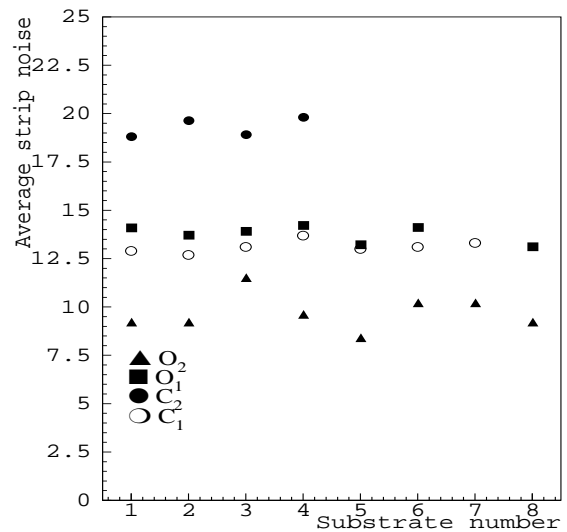

Figure 24: Variation of the average strip noise per substrate as a function of the substrate number, for modules O1, O2, C1 and C2.

19

average noise of the five detector modules without input resistors is 9.3±.5 ADC counts. Substrates 3 and 7 contain resistors but substrate 3 is partially broken. The noise of counters 3 and 7 is 11.5 and 10 ADC counts, respectively. Figure 22 shows that the signal to noise ratios of counters 3 and 7 in O2 are not significantly different from the ones obtained for counters with no series resistor. The conclusion is that the preamplifier protection offered by a 400 Ω resistor largely outweighs the increase in noise caused by this resistor.

7.7   Spatial resolution study

The distribution of residuals shown in figure 16 is too wide to be used to determine the MSGC spatial resolution as this is expected to be of the order of 40 μm. These large residuals between the silicon telescope prediction and the MSGC measurement are to be attributed to uncorrelated vibrations of the two detectors sitting on different benches, together with an unfavourable level arm.

Tracks were reconstructed using the measurements in two MSGC modules just before and after a third module. The prediction for the impact point in the central module is then compared to the measurement in that module. In this analysis, the information from the silicon telescope is only used to determine the coordinate along the strips in order to find the appropriate anode pitch. This procedure is applied after alignment of each concerned MSGC detector with respect to the telescope. A typical distribution of residuals obtained in this way for module O2 is shown in figure 25. The standard deviation of 52 μm corresponds to an MSGC spatial resolution of about 40 μm assuming
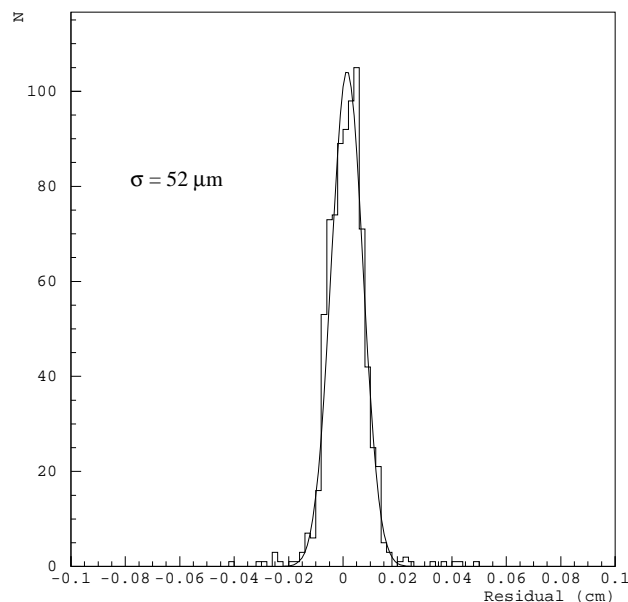

Figure 25: Difference between the Y coordinate of the impact point of beam particles with module O2, measured by module O2 and extrapolated from measurements in modules O1 and C1. The appropriate anode pitch is determined with the help of the silicon telescope.

the same resolution in all three modules. This estimation is corrected neither for mutiple scattering nor for the error coming from the way the pitch is obtained. However both contributions are expected to be negligible.

Figure 26c shows the spatial resolution measured for module O2 as a function of the anode pitch. The result of 38 μm obtained for a pitch of 218 μm is compatible with the spatial resolution measured for counters with parallel strips and an anode pitch of 200 μm, filled with a Ne/DME-50/50% gas mixture: 36±2 μm [22]. The spatial resolution degrades only to 44 μm for the largest anode pitch measured, of 240 μm, which is still quite acceptable for the tracking in CMS. These results are in agreement with a preceding measurement done for a trapezoidal counter [23]. Figure 26a shows the cluster size as a function of the anode pitch for modules O1, O2, O3, C1 and C2. Except for O3 working at a lower signal to noise because of their important leakage current, the cluster size is 2.3 strips in average. For module O4 shown in figure 26c, it is 3.6. This difference was already discussed in section 7.4. For all modules the cluster size does not vary significantly with the anode pitch.
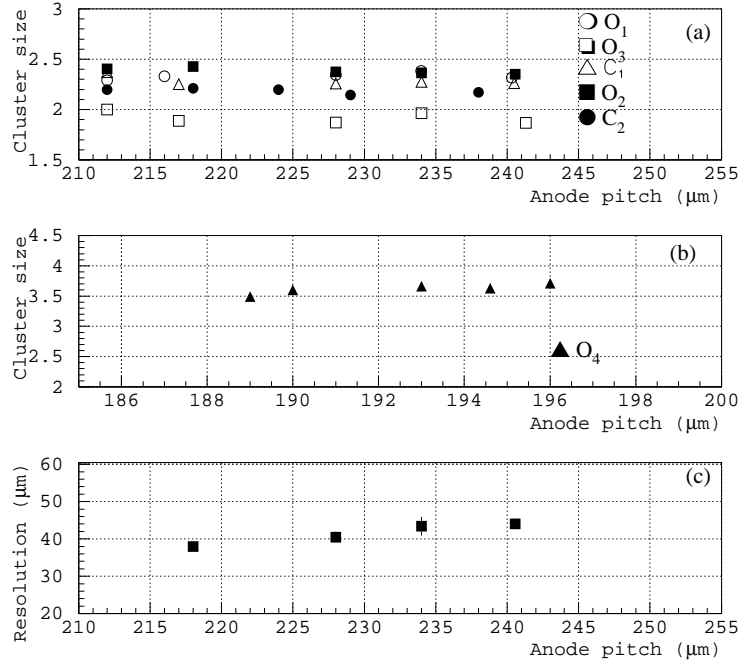
Figure 26: Variation of the cluster size (a) and (b) and of the spatial resolution (c), as a function of the anode pitch.

7.8   Alignment study

All counters in a given module need to be precisely aligned with respect to the gas box ($\simeq$30 μm). Optical alignment was performed for the "open" design modules (see section 3.1). The relative alignment of two neighbouring substrates was tested for two "open" design modules, O1 and O2.

A given substrate of each module is first aligned with respect to the silicon telescope, using the procedure described in section 7.3. The histograms to the left of figure 27(28) show for the aligned counter of O1(O2) the distribution of the difference between the Y coordinate of the beam impact point with this module calculated with the telescope information only, and the Y coordinate calculated with the n_{strip} value measured by the MSGC module, expressed in number of strips, for two anode pitches. The distributions to the right of these figures show the distributions of the same quantities for the neighbouring substrate, estimated without modifying the alignment parameters, assuming that the strips of both substrates point to a common point and that the distance between the last anode of the substrate to the left and the first anode of the substrate to the right, is twice the nominal anode pitch. A broadening of the distribution is observed together with a shift of the average value. Converted in μm this shift is of: 67 μm and 43 μm for O1 and 0 and -39 μm for O2. As an example, for O1 at a pitch of 237 μm, a rotation of 90 mrad is needed to also align the right counter, in addition to the shift of 43 μm in Y. These results signify that the optical alignment used here is not accurate enough and a final alignment with particles is necessary.

For the "closed" design, a fiber scan controlled machine is used to automatically position the substrates within a module. The lack of statistics with beam particles hitting the common edges of two neighbouring good substrates of module C1, prevents us to test that system with the data taken. However, after the beam test, the position of the substrates in C1 module was checked using an independant coordinate measuring machine. These measurements show that with this method, it is possible to position the substrates with a precision around 5 μm [24].

7.9   Edges study

The dead space expected between two modules may be studied with module C1 made of two half modules with four counters each, the beam hitting the edge counters of the two half modules. The tracks are reconstructed using the silicon telescope. Figure 29 shows the relation between extrapolated and measured strip number for particles hitting the two halves of module C1. Two peaks separated by about 8 mm are clearly observed. They correspond to the different alignment shifts needed for the two half modules and thus to the distance between the two counters. Taking
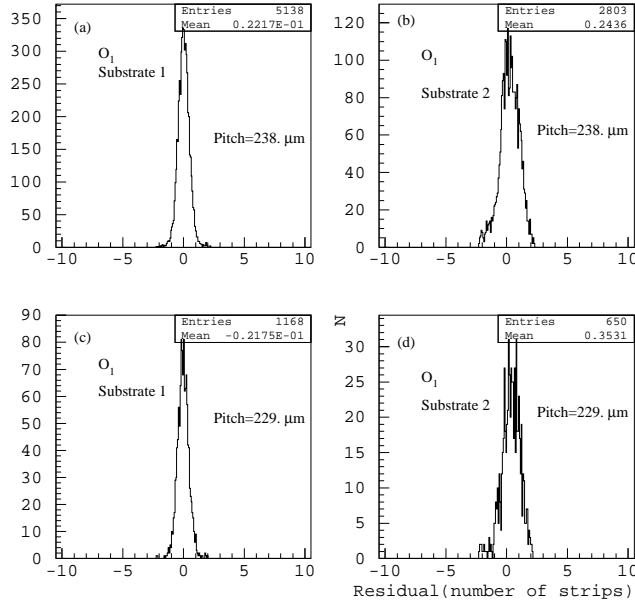
21

Figure 27: Distributions of the difference between the Y coordinate of the impact point of beam particles with the six modules, calculated with the telescope information only, and the Y coordinate calculated using the n_{strip} value measured by the MSGC module. The distributions to the left are for a substrate of O1 aligned with the telescope, the distributions to the right for the neighbouring substrate. the results are shown for two different anode pitches
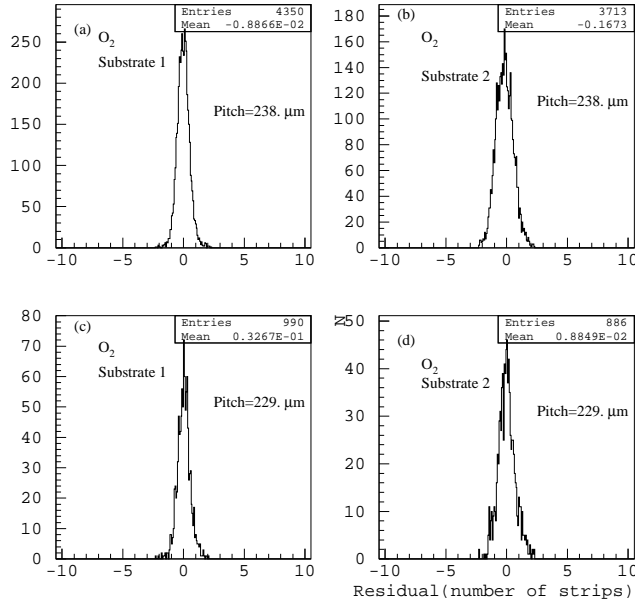

Figure 28: Distributions of the difference between the Y coordinate of the impact point of beam particles with the six modules, calculated with the telescope information only, and the Y coordinate calculated using the n_{strip} value measured by the MSGC module. The distributions to the left are for a substrate of O2 aligned with the telescope, the distributions to the right for the neighbouring substrate. The results are shown for two different anode pitches
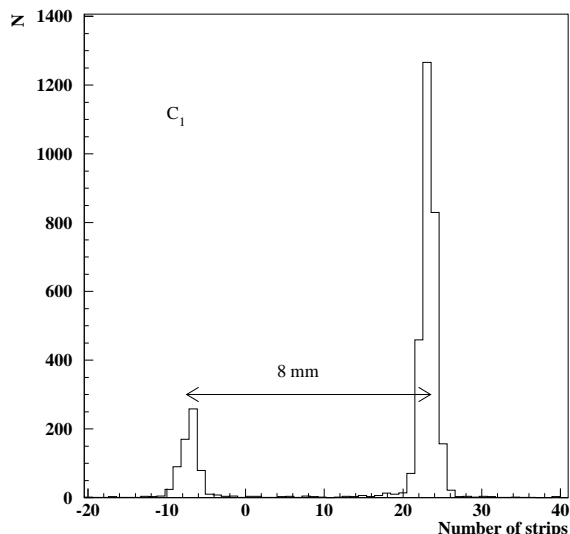
Figure 29: Relation between extrapolated and measured strip number for particles hitting the two halves of module C1.

into account the width of one half module, this corresponds to 2% dead space in the azimuthal angle ϕ. However for this milestone, the C1 4-fold half modules were not mounted on disks in the way described in reference [1]. The two half modules had to be fixed on a support identical to these used for the "open" design modules. It is hoped to decrease this dead space to 1.16% for the inner ring and 1.44% for the outer ring [1].

Following the various accidents and mistakes that occured during the construction many counters are damaged and only three pairs of adjacent counters were observed with all strips in good condition near the common edge. As no data were taken for these three regions with the $2X2cm^2$ scintillator trigger selecting beam particle traversing the silicon telescope, it was not possible to measure the dead space between two adjacent counters in the present milestone. However this dead space was measured to be negligible for the same configuration in reference [9].

The fact that there are only three good pairs of adjacent counters on a total of 32 that should be present, in principle, brought some suspicion that the region near the edges of adjacent counters might be dangerously more fragile. This was not observed in the Hermes MSGC tracker [10]. However, if one removes all pairs in which at least one of the counters is bad on a large area, and all pairs for which no data were taken, there are three good edge regions on a total of 13 good pairs which is still worrying. Again this bad score could be due to the overall bad quality of many counters. Indeed the fraction of dead strips among the twice four strips near the edges of good pairs of adjacent substrates is $(25\pm5)\%$. For the twelve next strips of the same pairs, it is $(12\pm3)\%$. The difference is hardly statistically significant. However this potential problem needs to be watched in future tests.

8   Conclusions

Six sector modules of the CMS forward backward MSGC tracker were built by various institutions and were all operated together in the X5 muon beam in CERN.

Different designs were tried, belonging to the categories "open" and "closed" design. Both options were proven to be feasible. During the construction, we learned how to avoid some problems encountered at the first attempts.Four protypes, belonging to both categories, had the same drift planes that prevented to raise the voltage higher than 2.7 kV in the milestone test described in this note. New drift planes, with lower resistivity, are now available and were proven to hold up to 3.8 kV in a more recent beam test.

The analysis of the data taken also do not allow to choose between the designs. A response with a gain dispersion of 11% standard deviation was observed both when going from one substrate to the next in a given module and when going from one module to another, excluding modules with an electronics problem (C2) or drawing too much current (O3). However this result should be tested with the final CMS performance substrates. Indeed the presence of coating could deteriorate the uniformity of the response.

It is also shown that the presence of a 400 Ω protection resistor between the anode strip and the readout electronics does not affect significantly the signal to noise ratio.

A scan along the strips of the trapezoidal counters also shows a constant gain, within 10%, for all modules but for the two modules for which the substrates were produced by OPTIMASK. This shows that the rule adopted for the relation between the anode-cathode distance and the varying anode pitch, allows to maintain a constant gain along the strips but might need modifications depending on the substrate production procedure.

For counters with no dead strips a detection efficiency of 97.5% is measured for an average signal to noise ratio starting at about 17. The spatial resolution in the trapezoidal counters is measured. It varies from 38 μm for a pitch of 218 μm to 44 μm for a pitch of 240 μm, which fullfills the requirements for the CMS tracker.

The alignment of the "open" design substrates was checked with beam particles. Shifts of up to 70 μm with respect to the nominal position were observed, together with rotation of 90 mrad. This would imply the measurement of the effective position for each substrate, in order to reach the required precision of 10 μm on the counters positionning. The lack of statistics prevented to test the alignment procedure of the "closed" design substrates with data but it was checked by a direct measurement after the beam test, showing a positionning precison of the order of 5 μm.

A dead space of 8 mm is observed between two contiguous "closed" half modules. This corresponds to 2% dead space in the azimuthal angle ϕ. It is hoped to reduce slightly that number when using the final mounting procedure of these modules onto disks.

A number of 38 substrates corresponding to a total of 19456 channels were present. However none of the six modules have all their counters in a state that is acceptable for a final production, except the second 4-fold half module of C1. These failures are not related to the type of design "closed" or "open" but can all be explained by mistakes done during the construction that will be avoided in the future. This demonstrates the difficulty to build such a system and the need for all institutions to gain experience with the final design. Since the test period it was decided to adopt the so called "Aachen closed design" as the construction requires less human intervention. As only one such module, C1, was present in the test beam, new prototypes of this type should be built by all institutions in order to gain experience, to improve the gas tightness, to test the alignment and to check the quality of the strips at the edge of adjacent counters with the new drift planes. Since the present milestone, one more closed module was successfully built and tested in the X5 beam, in September 1998.

The uniformity test, which was successfull here, should be repeated with the final substrates.

9   Acknowledgements

References

[1] CMS Technical Design Report Tracker, CERN/LHCC 98-6, CMS TDR 5

[2] ATLAS Internal note INDET-NO-076

[3] SRON, Space Research Organization, Utrecht, the Netherlands.

[4] NPP VOSTOK, Novosibirsk, Russian federation.

[5] OPTIMASK, 12 av. Ferdinand-de-Lesseps, 91420 Morangis,France.

[6] Baumer IMT Industrielle Messtechnik AG, Im Langacher, CH-8606 Greifensee, Switzerland

[7] L.L.Jones, PreMux specification, version 2.3, January 1995

[8] The forward-backward MSGC milestone status report. Belgium - France - Germany - Russia. IReS internal note, 23 r. du Loess, BP28 - 67037 Strasbourg Cedex 2.

[9] O. Bouhali et al.-Proc.Int. Workshop on MSGCs, Lyon 1995, p101.

[10] J.J. van Hunen, **Nucl. Instr. Meth. A 409** (1998) 95.

[11] Technical Design Report: A Possible Approach for the Construction of the CMS Forward-Backward MSGC Tracker, CMS NOTE-1997/081.

[12] Assembly of a closed module of 4 MSGC for the CMS forward tracker. M. Ageron et al., CMS-TN - 1998/022

[13] http://nicewww.cern.ch/sl/eagroup/beams.html#x5

[14] L. Celano *et al.*, **Nucl. Instr. Meth. A 381** (1996) 49-56.

[15] O. Toker *et al.*, **Nucl. Instr. Meth. A 340** (1994) 572.

[16] F. Drouhin, B. Schwaller et al., *A Unix SVR4–OS9 Distributed Data Acquisition for High Energy Physics*, UHA GRPHE, IEEE transaction for Nuclear Science, vol 5, 4 (1998).

[17] G. Claus et al., *Strip Detectors Read–Out System user's guide*, CRN 96–33, CNRS–IN2P3

[18] B.Schwaller, F.Drouhin, A.Pallares, J.C.Fontaine, Y.Benhammou, F.Charles, D.Huss, *The trigger system of the CMS barrel and forward milestones*, CMS Note 1998/029

[19] R.Brun and M.Goossens, *ZEBRA RZ Reference Manual*, Program Library Q100, CERN 1992.

[20] B. O. Baibusinov, *The Slow Control Modules specification*, Budker Institute for Nuclear Physics, Novosibirsk

[21] O. Bouhali *et al.*, **Nucl. Instr. Meth. A 378** (1996) 432.

[22] O. Bouhali *et al.*, **Nucl. Instr. Meth. A 413** (1998) 105.

[23] Spatial resolution of a wedge shaped MSGC module. S. Bachmann et al., CMS NOTE 1997/077.

[24] The Closed MSGC Design: Detectors and Mechanical Structure. S. Bachmann et al., PITHA 98/19 (Juni 1998).